PHYSICAL REVIEW B VOLUME 43, NUMBER 4 1 FEBRUARY 1991

Frank-Read source-activated flux shear in type-II superconductors

Alfred Kahan
Solid State Sciences Directorate, Rome Air Development Center, Hanscom AFB, Bedford, Massachusetts 01731
(Received 18 July 1990)

An expression is derived for the flux-pinning force density F_p as a function of magnetic induction B and pinning defect center density ρ, based on a model of flux-line-lattice shear activated by Frank-Read source dislocations. $F_p(b)$ peak positions shift with increasing ρ to larger b, where $b = B/B_{c2}$ is the reduced induction and B_{c2} is the upper critical field. For a given B there exists an optimum defect center density, ρ_{opt}, for which F_p becomes a maximum. The potential F_p enhancement is a function of the initial defect concentration ρ_i. At a constant B a larger F_p increase is obtained for smaller ρ_i, and at a constant ρ_i the increase is larger for larger B. Quantitative agreement for neutron-irradiated Nb_3Sn is obtained by fitting $F_p(b)$ data with three parameters ρ_i, a pinning defect center generating linear rate constant α, and the third consisting of a function of the Ginzburg-Landau κ and B_{c2}. The major characteristic of $F_p(b)$ for Nb_3Sn, which is F_p peaking at or near $b = 0.2$, is also true for the copper-oxide-based high-T_c superconductors, and the proposed model also applies to these materials.

INTRODUCTION

In previous publications[1,2] we discussed volume flux-pinning force density scaling laws for type-II superconductors derived from flux-line-lattice (FLL) shear mechanisms. The pinning force density is $F_p = J_c B$, where J_c and B are the critical current and the magnetic flux densities, respectively. A functional form for F_p was proposed by Fietz and Webb.[3] In their formulation, F_p is a product of separable variables consisting of the upper critical field B_{c2}, reduced magnetic induction $b = B/B_{c2}$, and a parameter related to material microstructure, the effective grain size D. Subsequent scaling laws proposed by Kramer,[4] Evetts and Plummer,[5] and Dew-Hughes,[6] introduce an additional parameter, the Ginzburg-Landau κ, and the variables are mathematically nonseparable.

In the Fietz-Webb formulation $F_p \propto b^p(1-b)^q$; that is, $F_p = 0$ at $b = 0$ and at $b = 1$, is continuous and positive between $0 < b < 1$, and peaks at $b_{\text{peak}} = p/(p+q)$. The two technologically prominent type-II superconductors, Nb_3Sn and Nb-Ti alloys, differ significantly in their microstructure and b_{peak}, indicating different mechanisms for flux pinning. Optimized bronze-processed multifilamentary Nb_3Sn has an equiaxed, or columnar, grain structure, $p = 0.5$, $q = 2$, and $b_{\text{peak}} \sim 0.2$, whereas for Nb-Ti alloys the microstructure is elongated grains, $p = q = 1$, and $b_{\text{peak}} \sim 0.5$. The shearing mechanism in Nb_3Sn is attributed to pin avoidance, and in Nb-Ti alloys to pin breaking. Hampshire and Jones[7] attempt to derive scaling laws applicable to both Nb-Ti and Nb_3Sn based on the same mechanism. Hampshire, Ikeda, and Chiang discuss scaling laws for $La_{1.85}Sr_{0.15}CuO_4$.[8] The F_p of high-T_c copper-oxide-based superconductors is similar to Nb_3Sn, having $b_{\text{peak}} \sim 0.2$.

Material processing or irradiation can alter the microstructure and change J_c. Effects owing to processing are usually discussed in terms of D, whereas irradiation effects are couched in terms of the pinning defect density ρ, defined by $\rho = 1/D^2$. For Nb_3Sn, West and Rawlings,[9] and Hascieck, Goringe, and Nourbakhsh[10,11] find a maximum in J_c as a function of D. J_c as a function of the neutron dose ϕ decreases at low magnetic fields, increases at higher fields, and at the higher fields it reaches a maximum and then decreases.[12,13] At a constant B, the J_c enhancement with dose is large for an initially low-J_c material, and is small for an initially high-J_c sample. At the higher fields it takes a larger dose to reach the maximum J_c. Another observation is that, with increasing dose, b_{peak} shifts to larger b.[14,15]

Based on these observations, an appropriate F_p scaling law has to predict that, at a constant B, there exists an optimum grain size D_{opt}, or optimum pinning defect center density ρ_{opt}, for which $J_c(D)$ becomes a maximum. Irradiation introduces damage and increases ρ. Irradiating up to ρ_{opt} will increase J_c, but irradiating to larger doses will decrease it. The scaling law should also predict that J_c enhancement or decrease is a function of the initial pinning defect center concentration ρ_i, and that for the same ϕ there is a larger J_c increase for low-J_c material. In Ref. 1 we showed that, for Nb_3Sn, qualitative agreement for processing changes and irradiation effects is obtained with the model proposed by Dew-Hughes,[6] which is a FLL shear mechanism activated by Frank-Read source dislocations.

In this paper we investigate further the FLL shear formalism applicable to Nb_3Sn and to the high-T_c superconductors. The $F_p(b)$ scaling laws proposed by Dew-Hughes, by Kramer, and by Evetts and Plummer, all contain a singularity which results in negative or infinite J_c at a finite b. For the Dew-Hughes model, the one we find most applicable to Nb_3Sn-type superconductors, we modify the Frank-Read source strength and eliminate the singularity. The modified model retains the main feature of the Dew-Hughes formalism, namely, the existence of

D_{opt}. We show, that, for Nb_3Sn, the calculated b_{peak} as a function of D span the experimentally observed range 0.17–0.28, and F_p is a maximum at $b=0.2$. For neutron irradiated Nb_3Sn, we find very good quantitative agreement between calculated and experimental $F_p(B)$.

FLUX-PINNING SCALING LAWS

Equations (1)–(3) list $F_p=J_cB$ for formalisms derived by Kramer,[4]

$$F_{pKramer}=\frac{1}{12\pi^2}\frac{D^2}{a_0(D-a_0)^2}C_{66}\ , \tag{1}$$

Evetts and Plummer[5] (EP),

$$F_{pEP}=\frac{1}{\pi}\frac{1}{(D-a_0)}C_{66}\ , \tag{2}$$

and Dew-Hughes[6] (DH),

$$F_{pDH}=\frac{1}{2\pi}\frac{\ln(D/a_0)}{D}C_{66}\ , \tag{3}$$

respectively. F_p (N m^{-3}) is the volume-pinning force density, J_c (A m^{-2}) is the critical current density, B (T) is the magnetic induction, D (m) is the effective grain size, C_{66} (N m^{-2}) is the shear modulus, and a_0 (m) is the fluxon spacing. For a triangular lattice,

$$a_0=(\tfrac{4}{3})^{1/4}(\phi_0/B)^{1/2}\ , \tag{4}$$

where ϕ_0 is the flux quantum. The three formulations have the same form, but differ in numerical coefficients and mathematical function relating D and a_0 to F_p. Approximate expressions for C_{66} are given by Labusch,[16]

$$C_{66\text{Labusch}}\simeq 3.6\times 10^4(B_{c2}/\kappa)^2(1-b)^2\ , \tag{5}$$

and by Brandt,[17]

$$C_{66\text{Brandt}}\simeq 1\times 10^5(B_{c2}/\kappa)^2 b(1-0.58b+0.29b^2)(1-b)^2\ , \tag{6}$$

where κ is the Ginzburg-Landau parameter. These formulations give six possible scaling laws for F_p: Kramer-Labusch, Kramer-Brandt, EP-Labusch, EP-Brandt, DH-Labusch, and DH-Brandt. In the defining equations, κ and B_{c2} occur as the factor $B_{c2}^{5/2}/\kappa^2$ and D as $DB_{c2}^{1/2}$. It is then convenient to plot and discuss these equations in terms of these combined parameters.

Figures 1 and 2 show $F_p(b)$, scaled by $\kappa^2 B_{c2}^{5/2}$, for selected $D^*\equiv DB_{c2}^{1/2}$ for Kramer-Labusch, EP-Labusch,

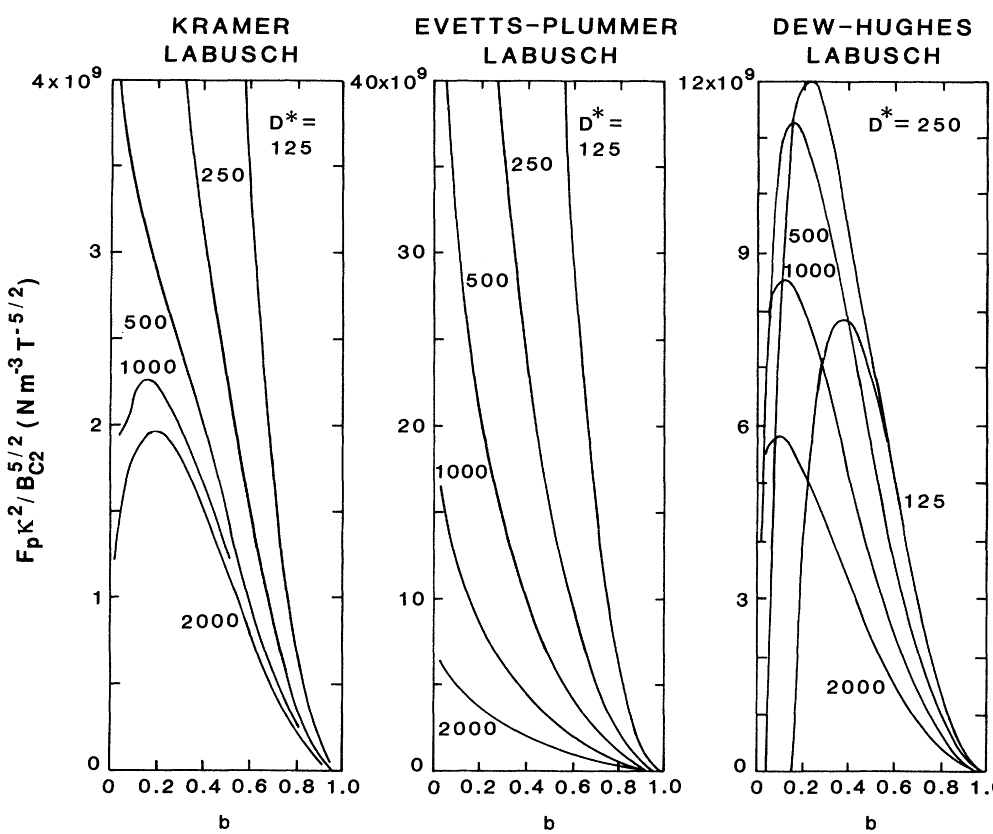

FIG. 1. Pinning force density F_p, scaled by $\kappa^2/B_{c2}^{5/2}$, as a function of reduced magnetic induction $b=B/B_{c2}$ for selected $D^*=DB_{c2}^{1/2}$, for flux-shear models of Kramer, Eq. (1); Evetts and Plummer, Eq. (2); and Dew-Hughes, Eq. (3). F_p was calculated using the shear modulus expression of Labusch, Eq. (5). κ is the Ginzburg-Landau parameter, D is the grain size in nm, and B_{c2} is the upper critical field.

DH-Labusch, and for Kramer-Brandt, EP-Brandt, DH-Brandt, respectively. F_p at $D = a_0$ is infinite for Kramer and EP, and is zero at a finite b for DH. In these figures, for clarity, we omit the branches for $D < a_0$. EP-Labusch has no peak for any D^*, and for Kramer and EP-Brandt, F_p peaks only for large D^*. For the same D^*, b_{peak} for Kramer and DH is larger with the Brandt than with the Labusch combination. For large grain sizes, $D \gg a_0$, Kramer-Labusch becomes independent of D and reduces to $F_p \propto b^{1/2}(1-b)^2$. For Kramer and EP, F_p at a given b is inversely proportional to grain size, $F_p \sim 1/D$, whereas for DH, F_p is an optimum at

$$D_{opt} = ea_0 = 2.72a_0 \ .$$

For DH-Labusch, $D^*_{opt} = 297 \text{ nm T}^{1/2}$ and F_p peaks at $b = 0.2$. For DH-Brandt, $D^*_{opt} = 210 \text{ nm T}^{1/2}$ and F_p peaks $b = 0.4$. Data showing F_p peaking as a function of D is consistent only with DH.

Figure 3 shows curves of b_{peak} as a function of D^* for the various formulations. For Kramer-Labusch, the lower b_{peak} limit is 0.086 and the upper limit asymptotically approaches 0.2, showing insensitivity to D. For Kramer-Brandt, the lower limit is 0.21 and the upper limit asymptotically approaches 0.4. EP-Labusch does not predict any b_{peak}. For EP-Brandt, the lower limit is 0.16 and the upper limit asymptotically approaches 0.30. For DH-Labusch, b_{peak} varies smoothly over a wide D^* range. For DH-Brandt, b_{peak} also varies smoothly over a wide range but the lower limit is 0.3. Consequently, only EP-Brandt and DH-Labusch have continuous b_{peak} values which span the $b = 0.2$ region applicable to Nb_3Sn. Curves labeled FR-Labusch and FR-Brandt will be discussed in the next section.

For Nb_3Sn, optimizing the fabrication process produces a finer grain structure and a larger B_{c2}, increases F_p, and shifts b_{peak} to larger values. Figure 3 shows that b_{peak} based on Kramer and EP increases, and based on DH decreases, with increasing D^*. Kramer and EP are then incompatible with experimental data. Based on these considerations, we choose DH-Labusch as the $F_p(b)$ scaling law which most closely describes superconductors with $b_{peak} \sim 0.2$.

FRANK-READ FORMALISM

In the previous section we showed that, for Nb_3Sn-type superconductors, DH-Labusch is in closest agreement with experimental $F_p(b)$. Dew-Hughes derived the expression for F_p by assuming that the FLL shear is activated by dislocations generated by a Frank-Read (FR)

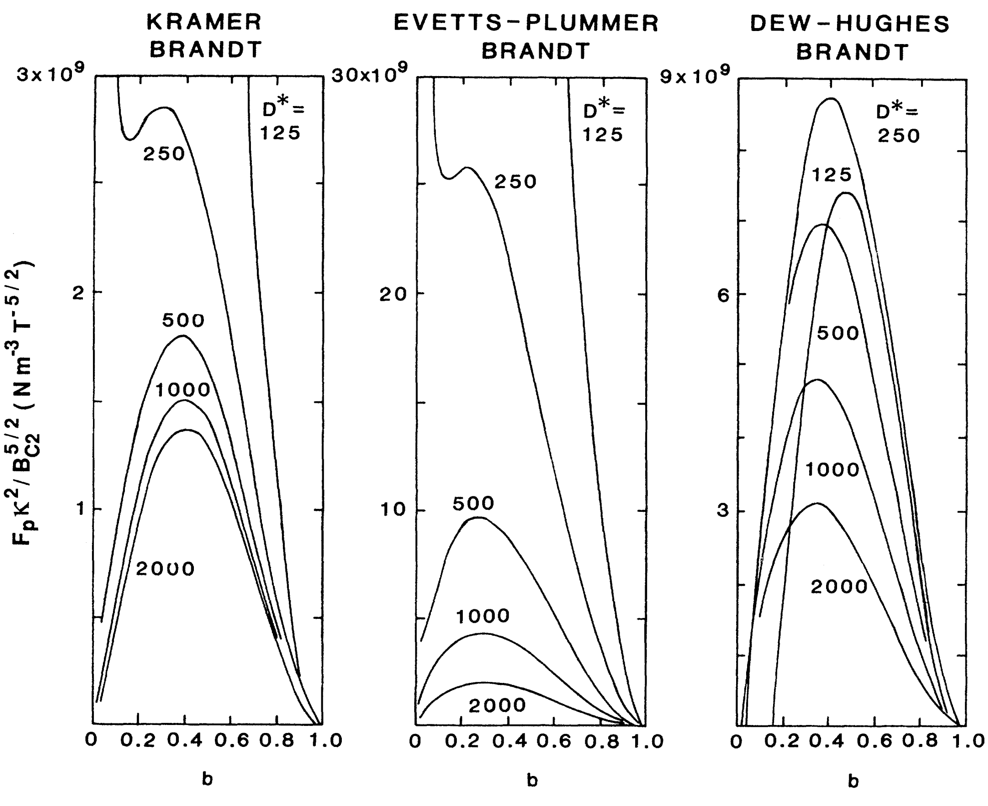

FIG. 2. Pinning force density F_p, scaled by $\kappa^2/B_{c2}^{5/2}$, as a function of reduced magnetic induction $b = B/B_{c2}$ for selected $D^* = DB_{c2}^{1/2}$, for flux-shear models of Kramer, Eq. (1); Evetts and Plummer, Eq. (2); and Dew-Hughes, Eq. (3). F_p was calculated using the shear modulus expression of Brandt, Eq. (6). κ is the Ginzburg-Landau parameter, D is the grain size in nm, and B_{c2} is the upper critical field.

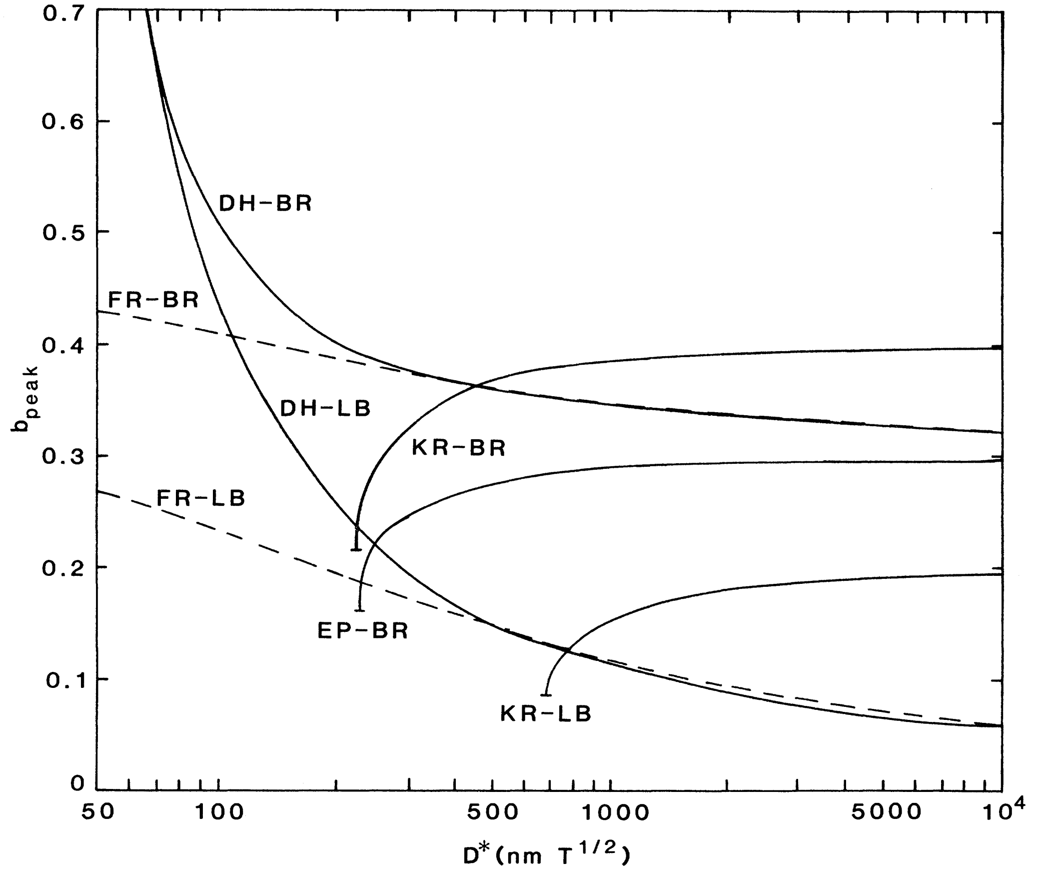

FIG. 3. $F_p(b)$ peak position b_{peak} as a function of $D^* = DB_{c2}^{1/2}$ for flux-shear models of Kramer (KR), Evetts and Plummer (EP), and Dew-Hughes (DH), using shear modulus expressions of Labusch (LB) and Brandt (BR). Curves labeled FR are defined by Eq. (8).

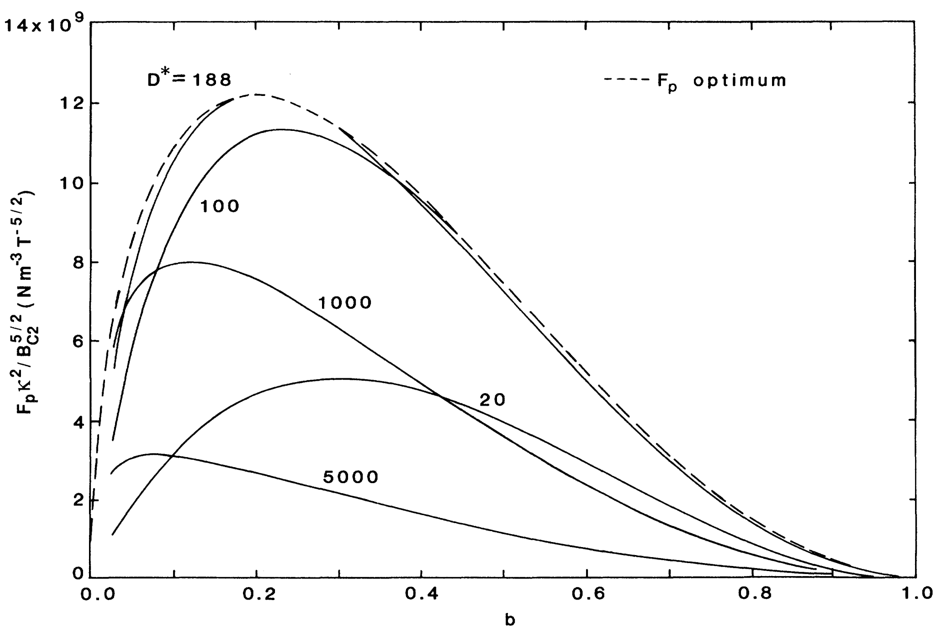

FIG. 4. Pinning force density F_p, scaled by $\kappa^2/B_{c2}^{5/2}$, as a function of reduced magnetic induction b for selected $D^* = DB_{c2}^{1/2}$ for the Frank-Read flux-shear model, Eq. (9). The dashed curve, Eq. (14), is the optimum F_p at a given b. κ is the Ginzburg-Landau parameter, D is the grain size in nm, and B_{c2} is the upper critical field.

source.[6] The critical stress τ is

$$\tau=(Gb^*/2\pi\Lambda)/\ln(\Lambda/b^*)\ , \tag{7}$$

where G is an appropriate modulus, b^* is the displacement Burgers vector, and Λ is the source length. Dew-Hughes also assumed that Λ is equal to the crystal grain size D, b^* is equal to the fluxon spacing a_0, and G is the shear modulus C_{66}. The volume-pinning force density $F_p=\tau/b^*$ is then the expression given in Eq. (3).

The principal difficulty with the DH model is that it allows F_p, and consequently J_c, to become negative for $D<a_0$. Dew-Hughes discusses this problem and suggests that, in these circumstances, one applies an effective grain size, a multiple of the microstructural grain size. The Dew-Hughes suggestion shifts the zero crossing to smaller b, but it does not eliminate the difficulty.

We propose a model which retains the basic features of DH, but at the same time insures that $F_p(b)$ is positive for all b. We suggest for the Frank-Read source length $\Lambda=D+a_0$. Substituting into Eq. (7),

$$F_p=\tau/b^*=\frac{C_{66}}{2\pi a_0}\frac{\ln(1+D/a_0)}{(1+D/a_0)}\ . \tag{8}$$

For $C_{66}=C_{66\text{Labusch}}$,

$$F_p=1.17\times10^{11}(B_{c2}^{5/2}/\kappa^2)b^{1/2}(1-b)^2\frac{ln(1+D/a_0)}{(1+D/a_0)}\ , \tag{9}$$

where

$$D/a_0=(DB^{1/2})/k=(D^*b^{1/2})/k=[(B/\rho)^{1/2}]/k\ , \tag{10}$$

and $k=48.9\times10^{-9}$ m T$^{1/2}$. We designate the F_p expression of Eq. (9) as FR-Labusch. A corresponding F_p expression using $C_{66\text{Brandt}}$ is designated as FR-Brandt. In the FR-Labusch formulation, the critical current density becomes

$$J_c=J_{c0}\frac{(1-b)^2}{(D/a_0)}\frac{\ln(1+D/a_0)}{(1+D/a_0)}\ , \tag{11}$$

where

$$J_{c0}=2.4\times10^{18}(B_{c2}/\kappa)^2D\ . \tag{12}$$

Figure 4 shows FR-Labusch, scaled by $\kappa^2/B_{c2}^{5/2}$, for selected D^*. F_p is positive at all b, and its highest maximum is at $b=0.2$ for $D^*=188$ nm T$^{1/2}$. For Nb_3Sn, $B_{c2}\sim20-25$ T and $\kappa\sim25$, and this D^* value corresponds to $D\sim40$ nm, and to a maximum $F_p\sim6\times10^{10}$ N/m^3 at $B\sim5$ T. Figure 4 also indicates that F_p at a constant b increases with D^*, reaches a maximum, and then decreases. For each b there exists an optimum D, D_{opt}, and a corresponding optimum F_p, $F_{p\,\text{opt}}$. This is shown as the dashed curve.

Figure 5 shows FR-Labusch normalized to its peak value for three D^* values. The solid circles represent the normalized Fietz-Webb scaling law,

$$F_p/F_{p\text{peak}}=3.5b^{1/2}(1-b)^2\ ,$$

peaking at $b=0.2$. The FR-Labusch curve peaking at $b=0.2$ closely agrees with the Fietz-Webb scaling law. Similar to DH, the b_{peak} shift to larger b with decreasing D^* or, equivalently, with increasing ρ. Figure 3, b_{peak} as a function of D^*, includes curves for the FR-Labusch and FR-Brandt combinations corresponding to $C_{66\text{Labusch}}$ and $C_{66\text{Brandt}}$, respectively. For FR-Labusch, the b_{peak} range is more limited than for DH-Labusch, but it still spans the range of interest to Nb_3Sn. FR-Labusch and DH-Labusch b_{peak} values are close for $D^*>500$ nm T$^{1/2}$,

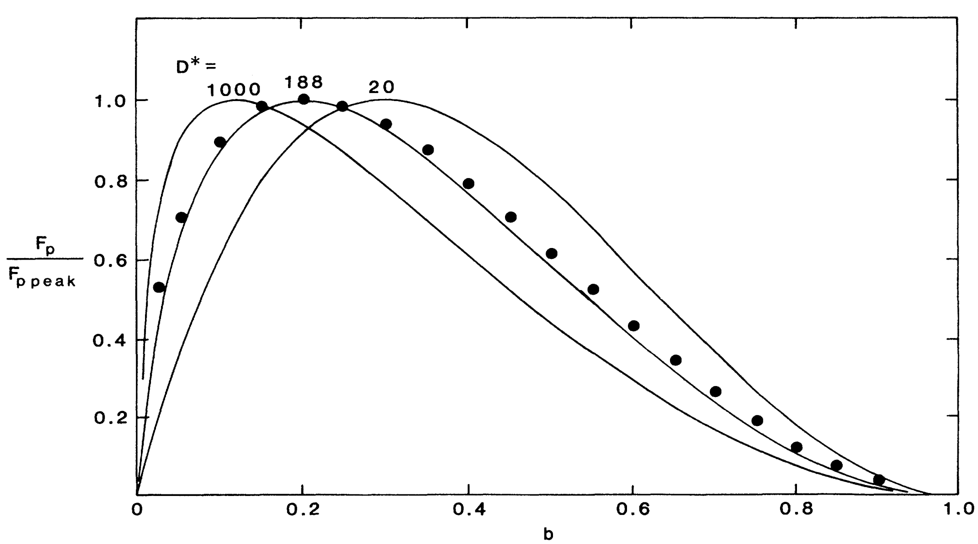

FIG. 5. F_p normalized to its peak value as a function of reduced magnetic induction b for selected $D^*=DB_{c2}^{1/2}$ for the Frank-Read flux-shear model, Eq. (9). The curve for $D^*=188$ nm T$^{1/2}$ peaks at $b=0.2$. The solid circles represent the normalized Fietz-Webb $F_p\propto b^{1/2}(1-b)^2$ scaling law. D is the grain size in nm, and B_{c2} is the upper critical field.

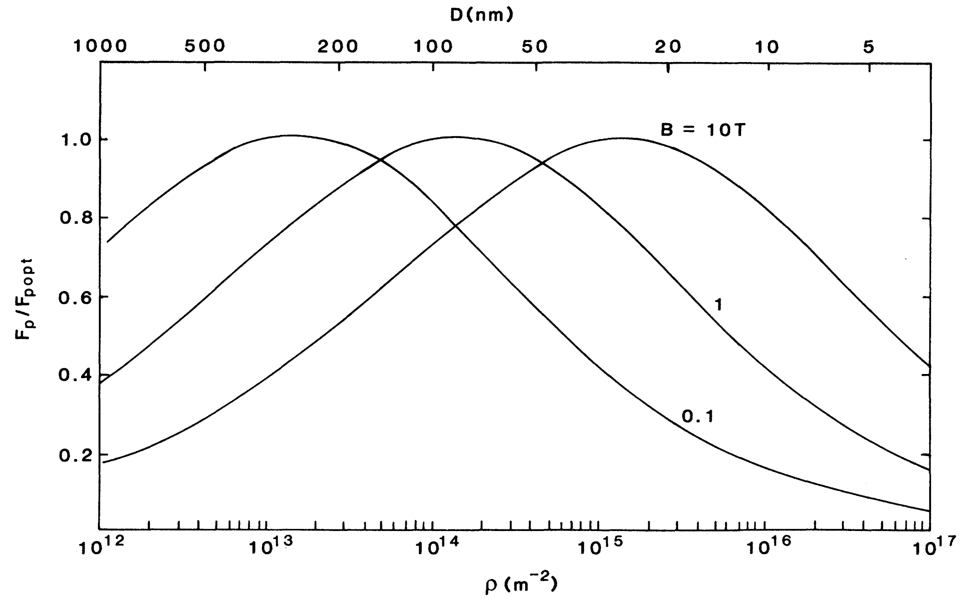

FIG. 6. F_p normalized to its optimum value, Eq. (15), as a function of pinning defect center density ρ for selected magnetic fields B. F_{popt}, Eq. (14), is the optimum-pinning force at a given B.

but at $b_{peak}=0.2$ their ratio is $D^*_{FR}/D^*_{DH}=\frac{188}{297}\sim\frac{2}{3}$. DH-Brandt and FR-Brandt b_{peak} lower limits approach 0.3, and neither of these are applicable to superconductors for which F_p peaks near $b=0.2$. Consequently, in our discussion of the proposed FR model, we imply FR-Labusch, as defined by Eq. (9).

OPTIMUM DEFECT DENSITY

Differentiating Eq. (9) with respect to D gives the optimum grain size D_{opt}, or optimum-pinning defect density ρ_{opt} (m^{-2}),

$$D_{opt}=(e-1)a_0=1.72a_0=84\times10^{-9}/B^{1/2}\ , \tag{13a}$$

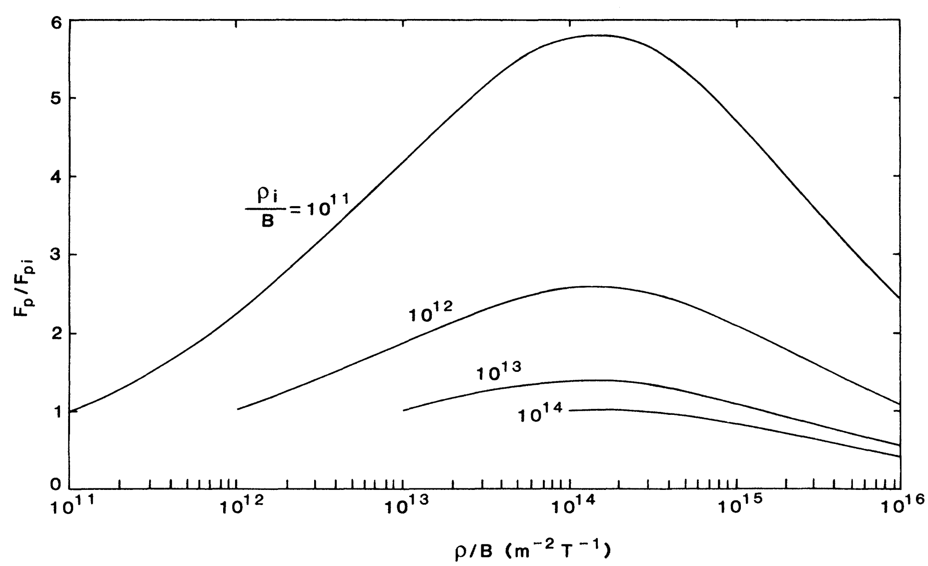

FIG. 7. F_p normalized to its initial value F_{pi}, Eq. (16), as a function of pinning defect center density ρ and initial pinning defect center density ρ_i. ρ and ρ_i are parametrized by magnetic field B. F_p/F_{pi} indicates the potential enhancement which can be obtained for a given ρ_i at a field B.

or

$$\rho_{\text{opt}} = 1.42 \times 10^{14} B \ . \tag{13b}$$

The corresponding optimum-pinning force density is

$$F_{p\text{opt}} = C_{66} / 2\pi e a_0 \ . \tag{14}$$

The dashed curve in Fig. 4 is a plot of $F_{p\text{opt}}$. F_p normalized to its optimum value is

$$\frac{F_p}{F_{p\text{opt}}} = \frac{e \ln(1+D/a_0)}{(1+D/a_0)} \ . \tag{15}$$

This normalization assumes that the factor $B_{c2}^{5/2}/\kappa^2$ is unaffected by the processing that changes the density of pinning centers.

Figure 6 shows $F_p/F_{p\text{opt}}$ as a function of ρ for magnetic-field values 0.1, 1, and 10 T. ρ_{opt} is a linear function of B, Eq. (13b), and the curves peak at 1.42×10^{13}, 1.42×10^{14}, and 1.42×10^{15} m^{-2}, respectively. As ρ increases, F_p increases for $\rho < \rho_{\text{opt}}$, peaks at $\rho = \rho_{\text{opt}}$, and decreases for $\rho > \rho_{\text{opt}}$. The enhancement increases with increasing B. For example, for ρ increasing from 5×10^{13} to 5×10^{14} m^{-2}, at 0.1 T, F_p decreases continuously; at 1 T, F_p increases, peaks, and then decreases; and, at 10 T, F_p increases continuously. Figure 6 also indicates that, for a given B, the F_p enhancement which can be obtained with increasing ρ, and whether one observes an F_p increase or decrease, depends on the initial defect density ρ_i, the density before material processing, for example, neutron irradiating. This is further illustrated in Fig. 7, where we plot the ratio of F_p to the initial pinning force density F_{pi} as a function of ρ/B for several ρ_i/B. It shows that, at a given B, one obtains a larger enhancement for a smaller ρ_i. For example, at B of 1 T, the maximum increase for $\rho_i = 10^{11}$ m^{-2} is 5.8 and for $\rho_i = 10^{13}$ m^{-2} it is only 1.4. At a constant ρ_i, the F_p increase is larger for larger B. For example, for $\rho_i = 10^{11}$ m^{-2}, the potential enhancement for $B = 0.1$ T is 2.6 and for 1 T it is 5.8.

DISCUSSION

Predictions for F_p based on FR-Labusch, Eq. (9), are in qualitative agreement with observed experimental features of Nb_3Sn as a function of processing and irradiation. For example, Brown *et al.*[12,13] report $J_c(B)$ measurements on several neutron-irradiated samples with different initial J_c values J_{ci}. They found that the fractional ratio J_c/J_{ci} decreased with neutron dose ϕ for small magnetic fields, but increased with higher fields. At the higher fields J_c/J_{ci} reached a maximum with ϕ, and then decreased with additional ϕ. The dose to reach the J_c/J_{ci} maximum increased with increasing B. They also showed that J_c/J_{ci} is a function of J_{ci}, with a low-J_{ci} sample substantially more enhanced by the same dose. All of these observations are in qualitative agreement both with DH-Labusch and FR-Labusch.

FR-Labusch contains two adjustable parameters, D or ρ, and κ, which can be determined by data fitting $F_p(B)$. The issues, difficulties, and results of such a fitting process are the same as those of DH-Labusch and were discussed in detail in Ref. 2. In Ref. 2 we also showed that very small changes in B_{c2}, variation within experimental accuracies, substantially affect D and κ values. Accurate B_{c2} values are difficult to measure, and therefore we suggested that B_{c2} should be treated as the third adjustable parameter. One obtains similar B_{c2} and κ values from $F_p(B)$ data sets fitted with either DH-Labusch or FR-Labusch, but derived D values are in ratio of $\sim\frac{2}{3}$.

In fitting a series of $F_p(B)$ curves as a function of ϕ, one would follow the same procedure: least-squares fit each set of experimental data with ρ, κ, and B_{c2}, and then find a relationship for $\rho(\phi)$, $\kappa(\phi)$, and $B_{c2}(\phi)$. We intended to perform such an analysis, but we have difficulties finding such data sets. However, we do find data sets for $J_c(\phi)/J_{ci}$ measured at several B.[12,13] From Eq. (9),

$$J_c/J_{ci} = F_p/F_{pi} = R\,(A_i/A)(\ln A)/(\ln A_i) \ , \tag{16}$$

where

$$R = (B_{c2}/B_{c2i})^{5/2}(\kappa_i/\kappa)^2 \ , \tag{17a}$$

$$A_i = 1 + (1/k)(B/\rho_i)^{1/2} \ , \tag{17b}$$

and

$$A = 1 + (1/k)(B/\rho)^{1/2} \ . \tag{17c}$$

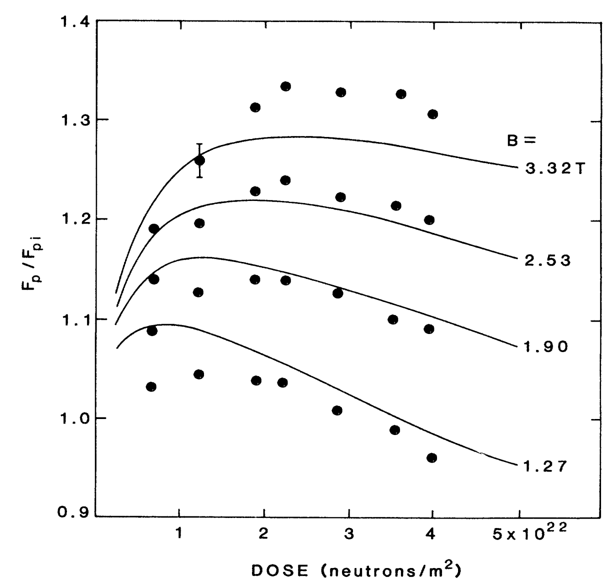

FIG. 8. F_p normalized to their initial values as a function of radiation dose and magnetic field for neutron irradiated Nb_3Sn. Experimental points of Brown *et al.*, Refs. 12 and 13. The curves, Eqs. (16)–(18), are calculated with parameter values $R = 1.0$, $\rho_i = 4.5\times 10^{13}$ m^{-2}, and $\alpha = 1.8\times 10^{-8}\, n^{-1}$.

We assume that $\rho(\phi)$ saturates exponentially,

$$\rho(\phi)=\rho_i+(\rho_s-\rho_i)[1-\exp(-\alpha'\phi)] \; . \tag{18a}$$

For $\alpha'\phi \ll 1$, this is approximated by

$$\rho \simeq \rho_i+\alpha\phi-\beta\phi^2+\dots . \tag{18b}$$

ρ_s is the saturated defect density, and α, α', and β are pinning defect generating rate constants. For $R=1$, the data fitting procedure reduces to a three, or possibly even a two, adjustable parameter fit: ρ_i, ρ_s, and α'; ρ_i, α, and β; or just ρ_i and α. We attempted such a curve fit to the Brown *et al.*[12,13] intermediate-J_{ci} sample data, the sample with the most extensive data points. We find that ρ is a linear function of ϕ, and the data set can be fitted with $\rho_i=4.5\times10^{13}$ m^{-2} and $\alpha=1.8\times10^{-8}$ n^{-1}. The defect density after the maximum dose $\phi=4\times10^{22}$ n/m^2, has increased to $\rho=7.7\times10^{14}$ m^{-2}. Figure 8 shows the comparison between $F_p(\phi)/F_{pi}$ and the data points. We consider the results encouraging for a fit by only two parameters. Discrepancies in Fig. 8 are greatest at low doses.

One source of the discrepancy may be attributed to radiation effects on B_{c2} and κ. In fitting the data set we assumed that R, Eq. (17a), equals unity. This may not be the case. For Nb_3Sn, Snead and Parker[18] report a peak, $B_{c2}(\phi)/B_{c2i}=1.05$ for $\phi=1.5\times10^{22}$ n/m^2, and then a decrease to 0.70 for $\phi=3.1\times10^{23}$ n/m^2. Okada *et al.*[15] report a similar peak and a decrease to 0.82 for $\phi=1.5\times10^{23}$ n/m^2. Colucci and Weinstock[14] show an increase to 1.14 for $\phi=1.8\times10^{22}$ n/m^2. We can find no data regarding $\kappa(\phi)$. In Eq. (17a), B_{c2}/B_{c2i} is raised to the power of $\frac{5}{2}$, and κ_i/κ is squared. For Nb_3Sn, $B_{c2}\simeq\kappa$. If $\kappa(\phi)/\kappa_i$ has the same dose dependence as $B_{c2}(\phi)/B_{c2i}$, then the effective power dependence is reduced from $\frac{5}{2}$ to $\frac{1}{2}$. However, if $\kappa(\phi)$ and $B_{c2}(\phi)$ dependencies are inversely proportional, then the effective power dependence is enchanced to $\frac{9}{2}$, and the effects can be considerable. The basic uncertainty in this fitting is due to the fact that the largest B for which measurements were performed was 3.32 T; that is, fields for which $b<0.2$. It is not possible to determine accurate or even approximate B_{c2} values from $J_c(B)$ limited to $b<b_{\rm peak}$. Since B_{c2} is undetermined, κ too becomes undetermined and $J_c(B)$ cannot be fitted with unique parameter values.

In lieu of experimentally determined $R(\phi)$, we refitted the data with R as an adjustable parameter. Figure 9 shows the comparison between F_p/F_{pi}, calculated with parameter values $R=0.76$, $\rho_i=1.2\times10^{13}$ m^{-2}, and $\alpha=1.5\times10^{-8}$ n^{-1}, and the Brown *et al.* data points. The fit is considerably improved, both in curve shape and in magnitude. For this limited ϕ-range, $R(\phi)$=const seems to be a good approximation.

To the best of our knowledge the results shown in Fig. 9 are the first reasonable comparisons between calculated and experimental $F_p(\phi,B)$. They indicate that the proposed model should be considered a viable formalism for Nb_3Sn-type superconductors.

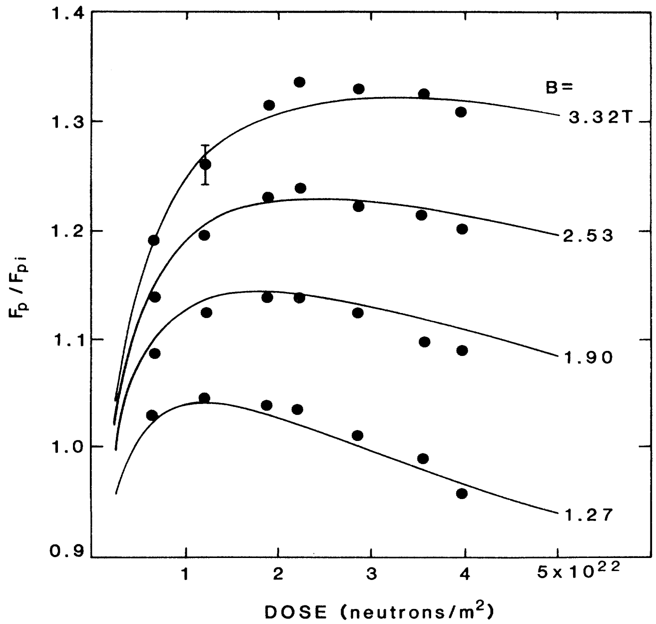

FIG. 9. F_p normalized to their initial values as a function of radiation dose and magnetic field B for neutron irradiated Nb_3Sn. Experimental points of Brown *et al.*, Refs. 12 and 13. The curves, Eqs. (16)–(18), are calculated with parameter values $R=0.76$, $\rho_i=1.2\times10^{13}$ m^{-2}, and $\alpha=1.5\times10^{-8}$ n^{-1}.

CONCLUSIONS

We have derived an expression for the flux-pinning force density F_p as a function of magnetic induction B, based on a mechanism of flux-line-lattice shear activated by Frank-Read source dislocations. We assume that the source length is given by $D+a_0$, where D is an effective microstructural grain size and a_0 the fluxon spacing. The formalism predicts that $F_p(b)$, where $b=B/B_{c2}$ and B_{c2} is the upper critical field, is continuous and positive between $0<b<1$, and peaks at some b value. The F_p peak position $b_{\rm peak}$ shifts with increasing pinning defect density ρ to larger b, $\rho=1/D^2$, and $F_p(b)$ achieves its maximum value at $b_{\rm peak}=0.2$. The results are in agreement with data for Nb_3Sn and for the copper-oxide-based high-T_c superconductors. The calculated $b_{\rm peak}$ as a function of D span the b range observed for these superconductors. For $b_{\rm peak}=0.2$, predicted field dependences are in close agreement with the Fietz-Webb scaling law $F_p\sim b^{1/2}(1-b)^2$.

For a given B there exists an optimum D, or defect density $\rho_{\rm opt}$, at which F_p is optimum. For a given ρ increment, F_p enhancement increases with increasing B. The potential F_p enhancement which can be obtained, and whether one observes any F_p increase at all, is a function of the initial defect concentration ρ_i. At a constant B, a larger increase is obtained for smaller ρ_i, and at a constant ρ_i, the increase is larger for larger B.

$F_p(B)$ predictions of the proposed model are in qualitative agreement with major experimental features. $F_p(B)$ contains three adjustable parameters, D or ρ, B_{c2}, and the

Ginzburg-Landau κ, which can be determined from least-squares fitting a specific data set. For neutron-irradiated Nb_3Sn very good quantitative agreement is obtained for $F_p(\phi)$ with three adjustable parameters ρ_i, pinning defect generating linear rate constant α, and a constant involving ratios of κ and B_{c2}.

ACKNOWLEDGMENTS

The author thanks his colleague F. Euler for his kind collaboration, and Dr. M. Alexander and Dr. A. Drehman for comments and discussions. The author also thanks Professor D. Dew-Hughes for helpful discussions.

[1]A. Kahan, Philos. Mag. Lett. **60**, 213 (1989).
[2]A. Kahan, Cryogenics **30**, 678 (1990).
[3]W. A. Fietz and W. W. Webb, Phys. Rev. **178**, 657 (1969).
[4]E. J. Kramer, J. Appl. Phys. **44**, 1360 (1973).
[5]J. E. Evetts and C. J. G. Plummer, in *Proceedings of the International Symposium on Flux Pinning and Electromagnetic Properties of Superconductors,* edited by T. Matsushita, K. Yamafuji, and F. Irea (Fukuoka, Matsukuma, 1985), pp. 146–151.
[6]D. Dew-Hughes, Philos. Mag. B **55**, 459 (1987).
[7]D. P. Hampshire and H. Jones, J. Phys. C **21**, 419 (1987).
[8]D. P. Hampshire, J. A. S. Ikeda, and Y.-M. Chiang, Phys. Rev. B **40**, 8818 (1989).
[9]A. W. West and R. D. Rawlings, J. Mater. Sci. **12**, 1862 (1977).
[10]Y. S. Hascicek, S. Nourbakhsh, and M. J. Goringe, Philos. Mag. B **59**, 405 (1989).
[11]Y. S. Hascicek, M.J. Goringe, and S. Nourbakhsh, Philos. Mag. B **59**, 423 (1989).
[12]B. S. Brown, T. H. Blewitt, D. G. Wozniak, and M. Suenaga, J. Appl. Phys. **46**, 5163 (1975).
[13]B. S. Brown, T. H. Blewitt, T. L. Scott, and M. Suenaga, J. Appl. Phys. **49**, 4144 (1978).
[14]S. L. Colucci and H. Weinstock, J. Nucl. Mater. **72**, 142 (1978).
[15]T. Okada, M. Fukumoto, K. Katagiri, K. Saito, H. Kodaka, and H. Yoshida, J. Appl. Phys. **63**, 4580 (1988).
[16]R. Labusch, Phys. Status Solidi **32**, 439 (1969).
[17]E. H. Brandt, Phys. Rev. B **34**, 6514 (1986).
[18]C. L. Snead and D. W. Parkin, Nucl. Technol. **29**, 264 (1976).